FOA
DEFENCE RESEARCH ESTABLISHMENT

FOA-R--99-01267-311--SE
October 1999
ISSN 1104-9154

Test report

Hakur Ingason, Per Werling

Experimental Study of Smoke Evacuation in a Model Tunnel

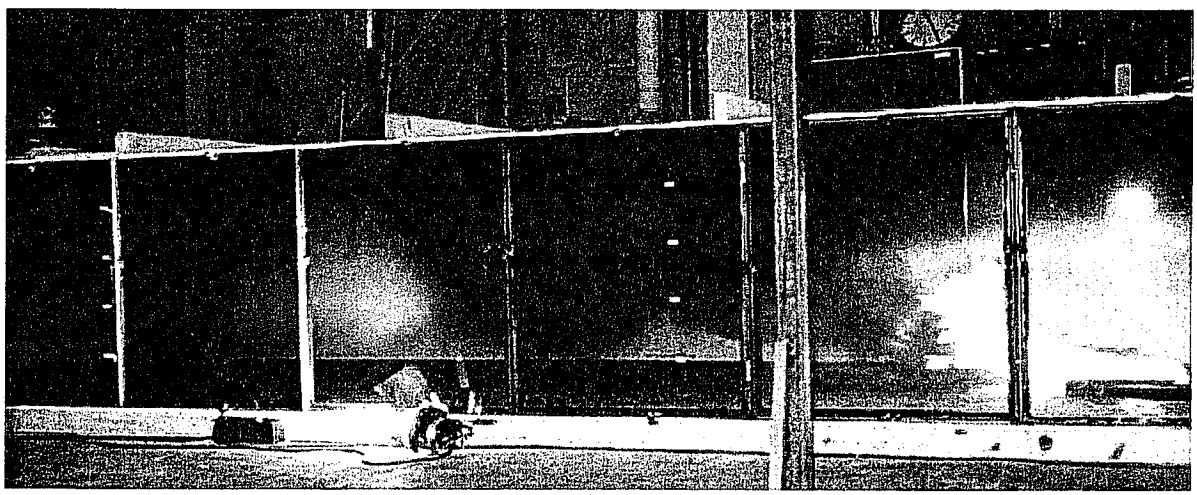

403 - 981
Brandforsk projekt

Weapons and Protection Division
SE-147 25 TUMBA

DEFENCE RESEARCH ESTABLISHMENT
Weapons and Protection Division
SE-147 25 TUMBA
SWEDEN

FOA-R--99-01267-311--SE
October 1999
ISSN 1104-9154

Haukur Ingason, Per Werling

Experimental Study of Smoke Evacuation in a Model Tunnel

Distribution: FORT, SkyddS, SRV, KTH, LTH, Brandförsvarsföreningen, SP, Vattenfall, Telia, Vägverket, Brandkonsulten AB, SCC Safety Engineering, Brandskyddslaget, Brandforsk.
FOA: Inst 23

Issuing organization	Document ref. No., ISRN	
Defence Research Establishment Weapons and Protection Division SE-147 25 TUMBA SWEDEN	FOA-R--99-01267-311--SE	
	Date of issue October 1999	Project No. E2761
	Project name (abbrev. if necessary) Experimental Study of Smoke Evacuation in a Model Tunnel	
Author(s) Haukur Ingason, Per Werling	Initiator or sponsoring organization Swedish Fire Research Board	
	Project manager Per Werling	
	Scientifically and technically responsible	

Document title

Experimental Study of Smoke Evacuation in a Model Tunnel

Abstract

The present study show the influence of longitudinal ventilation on the efficiency of thermal and mechanical point exhaust ventilation in tunnels.

Smoke spread were documented along a model tunnel measuring 20 m long, 2 m wide and 1 m high. The cross-section (1 x 2 m) is about 1:8 of a full-scale road tunnel. One side of the tunnel consisted of a fire resistant window glass. The window (20 m) was used to visually observe and document the smoke spread. The visibility in the smoke was measured at various locations using optical density meters. Temperatures, velocities, mass flow rates and radiation along the tunnel were also measured. These data can be used for validation of CFD codes. The fire source was stationary and each test was run for 12 minutes.

The fire size varied from 30 to 80 kW, which corresponds to full-scale fires of 5 to 15 MW. The fuel for the pool fire was kerosene. The ventilation arrangement and the longitudinal velocities were varied. Exhaust shafts were mounted along the tunnel, both thermal and mechanical. The exhaust flow rate varied between 0.1 m^3/s to 2.7 m^3/s which corresponds to 18 m^3/s to 488 m^3/s in full scale. The longitudinal velocities ranged from 0 to 2 m/s, which corresponds 0 to 5.6 m/s in full scale.

Keywords tunnel, fire, smoke, longitudinal ventilation, exhaust ventilation, visibility, optical density, model tunnel, mass flow rate

Further bibliographic information	Language English	
ISSN 1104-9154	ISBN	
	Pages 28	Price Acc. to pricelist

Distributor (if not issuing organization)

Dokumentets utgivare	Dokumentbeteckning, ISRN	
Försvarets forskningsanstalt Avdelningen för Vapen och skydd SE-147 25 TUMBA	FOA-R--99-01267-311--SE	
	Dokumentets datum Oktober 1999	**Uppdragsnummer** E2761
	Projektnamn (ev förkortat) Experimentell studie av rökevakuering i en modelltunnel	
Upphovsman(män) Haukur Ingason, Per Werling	**Uppdragsgivare** Styrelsen för svensk brandforskning	
	Projektansvarig Per Werling	
	Fackansvarig	

Dokumentets titel i översättning

Experimentell studie av rökevakuering i en modelltunnel

Sammanfattning

Påverkan av längsventilation och effekten av termisk och mekanisk punktutsug via schakt i en modelltunnel studerades i denna rapport.

Brandgasspridningen är dokumenterad och kvantifierad längs en 20 m lång, 2 m bred och 1 m hög modelltunnel. Tvärsnittsarean (1 x 2 m) motsvarar 1:8 av en fullskalig vägtunnel. Ena sidan av tunneln (20 m) var försedd med värmetåligt glas, detta för att kunna observera och dokumentera brandgasspridningen. Optisk täthet i brandgasen, temperatur, hastighet, syrekoncentration, förbränningshastighet och värmestrålning blev registrerad på ett antal ställen i tunneln. Brandförloppet var stationärt och försöken pågick i 12 minuter.
Dessa data kan användas för validerig av CFD koder.

Brandeffekten varierade från 30 till 80 kW, vilket motsvarar 5 till 15 MW i fullskala. Fotogen användes som bränsle i brandkärlet. Ventilationsschakten och lufthastigheten i tunneln varierades.
Både termiska och mekaniska ventilationsschakt var monterade längs tunneln.

Nyckelord tunnel, brand, rök, längsventilation, brandgasventilation, sikt, optisk densitet, modelltunnel, förbränningshastighet

Övriga bibliografiska uppgifter	**Språk** Engelska	
ISSN 1104-9154	**ISBN**	
	Omfång 28	**Pris** Enligt prislista

Distributör (om annan än ovan)

V.1.3

Table of content

1 Introduction

The generation of smoke in fires is generally associated with reduction in visibility and exposure to toxic environments. In fires, reduction in visibility due to smoke often leads to a critical situation for escaping people. Due to toxic gases and high temperatures the situation may be very hazardous if people are not quickly able to find their way to a safe place. This was also the case in the Mont Blanc fire disaster where over 40 people died.

Since CFD models are commonly used in the design of escape routes in tunnels a reliable smoke model is essential. There is still a great lack of experimental data for verification of smoke spread calculations using CFD, especially in tunnels. The main objective of present study was to investigate the influence of longitudinal ventilation on the efficiency of thermal and mechanical ventilation in tunnels using exhaust shafts and to obtain experimental data for comparison with CFD models. CFD models calculate numerically the conservation of mass, momentum and energy in an arbitrary number of control volumes. The number of control volumes typically ranges from thousands up to several hundred thousands.

The main objective of present study was to investigate the influence of longitudinal ventilation on the efficiency of thermal and mechanical ventilation in tunnels using exhaust shafts and to obtain well defined experimental data for validation of CFD models. Totally thirtysix tests were performed, twenty six with thermal ventilation and ten with mechanical ventilation.

2 Experimental set-up

Smoke spread tests were performed in a model tunnel measuring 2 m wide, 1 m high and 20 m long. The material of the walls, floor and ceiling consisted of a 12 mm Promatec fibre-silica board - except for one side-wall which consisted of 5 mm thick fire resistant window glass. The window was used to visually document the smoke spread. The fire load consisted of a Kerosene pool fire located 2.5 m from one end of the tunnel. Two different pan sizes were used, 0.33 x 0.33 m and 0.4 x 0.4 m, respectively. The exhaust ventilation arrangement and the longitudinal velocity was varied. Different number of thermal shafts were mounted along the tunnel at locations A, B and C. Mechanical ventilation was arranged in shaft B in figure 1.

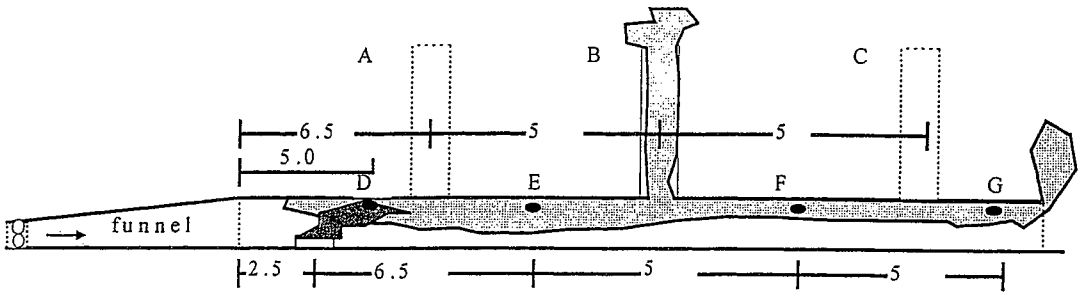

Figure 1 The experimental set-up. All dimensions are in metre.

A specially designed funnel shaped tunnel was attached to one end of the tunnel in order to create a uniform flow over the cross-section at the tunnel entrance, see Figure 1. The other end of the tunnel was fully open. Extensive work was put on creating a uniform air flow over the tunnel cross-section prior to the fire was ignited.

Measurements were performed at four different locations downstream of the fire, locations D, E, F and G, see Figure 1. The measuring points were placed at the centreline of the tunnel. The optical density was measured at E, F and G with optical density meters (photocell and lens) over the path length of 2 m. The optical density was converted to smoke concentration by divide the measured value with the smoke extinction coefficient 3300 m^2/kg [1]. The oxygen concentration was measured at E, F and G in a point at 0.25 m below ceiling and at the centreline of the tunnel. Oxygen concentrations (O_2) were measured by sucking the gases through a probe consisting of copper tube (Ø 6 mm) to an analyser. The thermocouples were of type K with a wire diameter of 0.25 mm, chromel-alumel, 1200 °C range and mounted at each station (D, E, F and G) at heights 0.1, 0.3, 0.5, 0.7, 0.8 and 0.9 m above the floor. The velocity was measured using bi-directional probes. They were placed 0.9 m above floor in station D, E, F and G and at 0.5 m above floor at station E and F.

In order to measure the mass burning rate the Kerosene fuel pan was placed on a weighing platform located under the floor (see figure 2). The floor consisted of a 12 mm Promatec silica board. The distance between the Promatec floor and the concrete floor of the test hall was 95 mm. Four 30 mm high stainless steel rods were put through the Promatec floor. Any friction to the Promatec boards was prevented by drilling the holes slightly wider than the rods. Any influence of heating on the results were not observed. The gas temperature close to the load cell did not increase more than 2 °C during the test. The accuracy of the load cell was +/- 1 g.

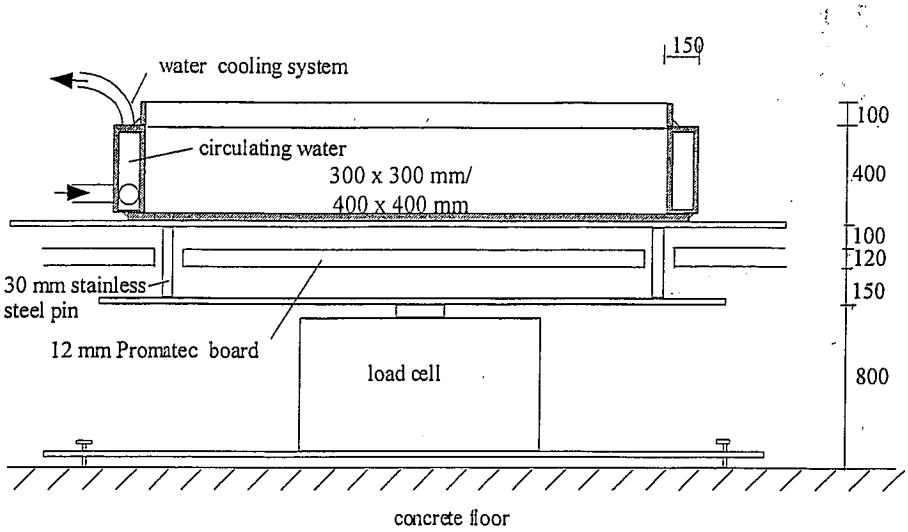

Figure 2 A cross-sectional view of the weighing platform and the fuel pan.

Extensive work was carried out to obtain a steady mass burning rate during the pool fire tests with Kerosine. Usually the rim of a fuel pan will be warmed up and the heat balance at the fuel surface will continuously change. This will result in a mass burning rate which is unsteady during the fire test. For small fuel pans used here this can be a great problem. The simplest way to obtain steady state conditions is by controlling the heat balance. This can be done by cooling the rim by circulate water. The problem is to find the appropriate geometry of the rim and an appropriate water flow rate.

After extensive work it was found that for the square pans used the best results were obtained with a water flow rate of 2 litre/minute and a cross sectional area of the rim by 15 mm wide and 50 mm high. The rim it self consisted of a square steel measuring 15 mm x 40 mm with either a 300 x 300 mm steel sheet or 400 x 400 mm (the bottom of the fuel pan) welded to the U-profiles. In order to avoid fuel leaking over the edge of the rim a 10 mm high steel edge was welded on the top of the rim. Thus, the height of the inner surface of the pan was 50 mm. The water cooled part was 40 mm. The thickness of the steel used in the rim was 2 mm. The temperature of the water flowing into the rim of the fuel pan was 10 °C and the water temperature flowing out from the rim was about 30 - 35 °C. In Figure 3, typical mass burning rate curves are shown for two different pan sizes. This method is found to be very robust and cheap. The mass burning rate became stationary after only 1-2 minutes.

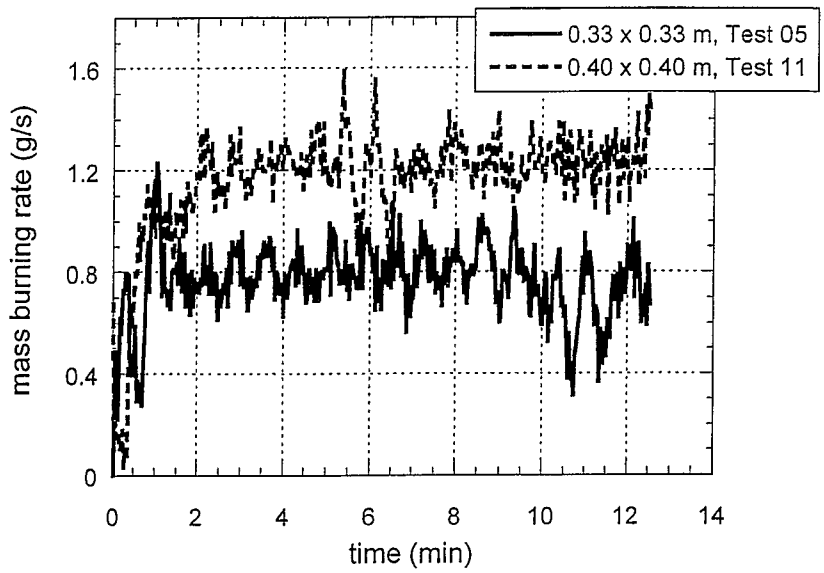

Figure 3 Mass burning rate of Kerosene measured with water cooled rims. Result using two different pan sizes are shown, 0.33 x 0.33 m and 0.40 x 0.40 m, respectively.

Every test was run for 12 minutes in order to obtain stationary conditions within the tunnel. It is difficult to obtain stationary wall temperatures but the gas temperatures were found to be quite stationary. In figure 4 a plot is given of the gas temperature and the ceiling temperature at location E. The ceiling temperature was measured by drilling a 11 mm deep hole in the Promatec board from the top. Thus 1 mm remained to the exposed surface at station E. The thermocouple was glued in the hole to obtain a good contact with the material. As can be observed in figure 4 the gas temperature (0.1 m from ceiling at E) is quite stationary whereas the ceiling is still warming up at the end of the test. All the average values presented in Appendix are taken from the 7^{th} to the 11^{th} minutes of the test.

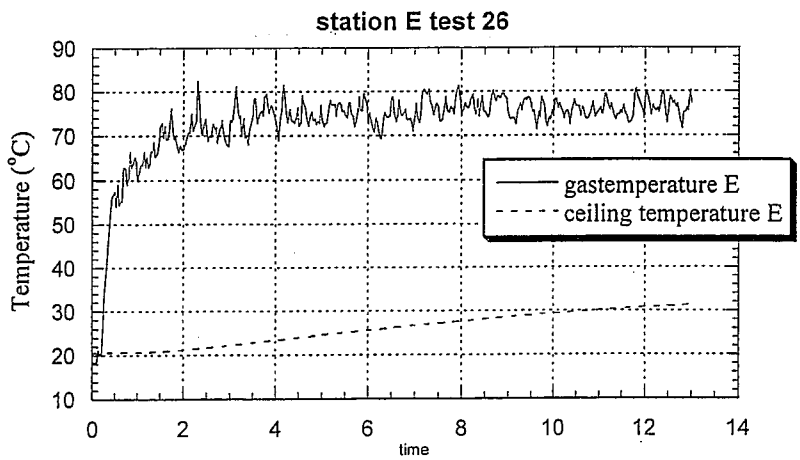

Figure 4 Gas temperature 0.9 m above floor and ceiling temperature 1 mm from the exposed ceiling surface at station E.

In order to establish a uniform flow a fan was attached to the tunnel, see Figure 1. The longitudinal ventilation (air velocity) inside the tunnel was varied. Five different air velocities were used in the test series, 0, 0.5, 0.75, 1 m/s and 2 m/s. These velocities correspond to 0, 1.4, 2.1, 2.8 and 5.6 m/s in a full scale (1:8) tunnel. This can be obtained by Froude scaling [2]. The following relationships for velocity (u), exhaust flow rate (V) and heat release rate (Q) can be found in the literature [2]:

$$u_F = u_M \sqrt{\frac{L_F}{L_M}} \tag{1}$$

$$V_F = V_M \left(\frac{L_F}{L_M}\right)^{5/2} \tag{2}$$

$$Q_F = Q_M \left(\frac{L_F}{L_M}\right)^{5/2} \tag{3}$$

These equations yields the full-scale results where index F is referring to full scale and M is referring to model scale. L is the length scale where L_F=8 and L_M=1.

Different arrangements of shafts were used in the test series. The number and size of the shafts were also varied. The thermal shaft was 3 m high which corresponds to 24 m in full scale. The mechanical shaft was 2 m high (16 m). Further, all figures in parenthesis corresponds to full scale values. The cross-section of the thermal shafts measured 0.4 x 0.4 m (3.2 x 3.2 m) and the mechanical shaft 0.6 x 0.6 m (4.8 x 4.8 m). The heat release rate, Q, was determined by multiplying the average mass burning rate with the heat of combustion of H_c=39.5 kJ/g. This value was obtained by direct measurement in a Cone Calorimeter [3].

Table 1 The experimental program using thermal shafts.

Test no	Air velocity (m/s)	Shaft (height/width)	Number of shafts	Fire source (m x m)	Average m_f (g/s)	Q (kW)
01	0	1/0.4	3	0.33 x 0.33	0.97	38.3
02	1	--- " ---	--- " ---	--- " ---	1.07	42.3
03	0	3/0.4	--- " ---	--- " ---	0.83	32.7
04	0.5	--- " ---	--- " ---	--- " ---	0.78	30.9
05	0.75	--- " ---	--- " ---	--- " ---	0.76	29.9
06	1	--- " ---	--- " ---	--- " ---	1.04	40.9
07	0	--- " ---	--- " ---	0.4 x 0.4	1.35	53.4
08	1	--- " ---	--- " ---	--- " ---	1.39	54.9
09	0.75	--- " ---	--- " ---	--- " ---	1.27	50.3
10	0.5	--- " ---	--- " ---	--- " ---	1.18	46.6
11	0.5	3/0.4	1	--- " ---	1.23	48.7
12	0.75	--- " ---	--- " ---	--- " ---	1.24	49.0
13	1	--- " ---	--- " ---	--- " ---	1.49	59.0
14	0	--- " ---	--- " ---	--- " ---	1.82	71.9
15	0.5	3/0.2	--- " ---	--- " ---	1.22	48.3
16	1	--- " ---	--- " ---	--- " ---	1.77	70.0
17	0	closed	0	--- " ---	2.01	79.4
18	1	--- " ---	--- " ---	--- " ---	1.45	57.4
19	0.75	--- " ---	--- " ---	--- " ---	1.25	49.2
20	0.5	--- " ---	--- " ---	--- " ---	1.31	51.8
21	0	--- " ---	--- " ---	0.33 x 0.33	0.86	33.9
22	1	--- " ---	--- " ---	--- " ---	1.04	41.0
23	0.75	--- " ---	--- " ---	--- " ---	0.76	29.9
24	0.5	--- " ---	--- " ---	--- " ---	0.77	30.3
25	0.5	3/0.6	--- " ---	0.4 x 0.4	1.30	51.3
26	1	--- " ---	--- " ---	--- " ---	1.41	55.9

Table 2 The experimental program for mechanical ventilation.

Test no	Air velocity (m/s)	Shaft (height/width)	Exhaust ventilation (m^3/s)	Fire source (m x m)	Average m_f (g/s)	Q (kW)
27	0	2/0.6	2	0.4 x 0.4	1.56	61.62
28	0	--- " ---	2.7	--- " ---	1.14	45.03
29	1	--- " ---	2.7	--- " ---	1.51	59.64
30	1	--- " ---	1.56	--- " ---	1.43	56.49
31	1	--- " ---	2	--- " ---	1.42	56.09
32	1	--- " ---	2.3	--- " ---	1.63	64.39
33	0.5	--- " ---	2	--- " ---	1.35	53.33
34	1	--- " ---	2.7	--- " ---	1.50	59.25
35	2	--- " ---	2	--- " ---	1.89	74.26
36	2	--- " ---	2.7	--- " ---	1.87	73.87

3 Experimental results

In the following experimental results are presented using thermal and mechanical ventilation. Experimental data is also presented in tabulated form in Appendix. The values given there are average values.

3.1 Smoke spread

The smoke spread in figures 5 a-j was documented with aid of rulers attached to the glazed window at various distances along the tunnel. The experiments show an area with dense smoke (hot layer) close to the ceiling, approximately 0 - 30 cm below the ceiling and an area with intermediate smoke concentrations (mixing layer) approximately between 30 - 60 cm below the ceiling. An area with none or very small concentrations of smoke (cold layer) was found between 0 - 40 cm above the floor. Estimated smoke concentration profiles in stations E, F and G are plotted in figures 5a-d. These profiles are based on visual judgement of smoke concentration over the tunnel height. The flow directions in the hot layer and the mixing layer regions are indicated in figures 5a-j. All figures in parenthesis corresponds to full scale values.

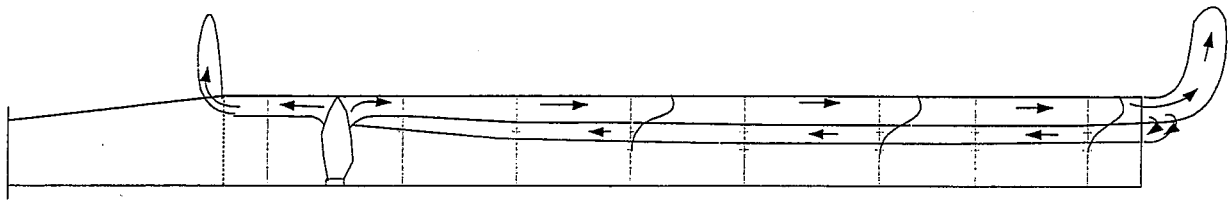

Figure 5a No longitudinal ventilation. Fire source 79.8 kW (14.4 MW). Estimated smoke concentration profile is given for station E, F and G (**test 21**).

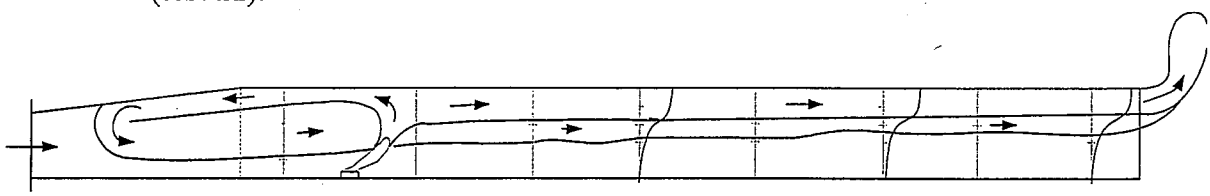

Figure 5b Longitudinal ventilation 0.5 m/s (1.06 m/s). Fire source 51.8 kW (9.4 MW) **(test 20).**

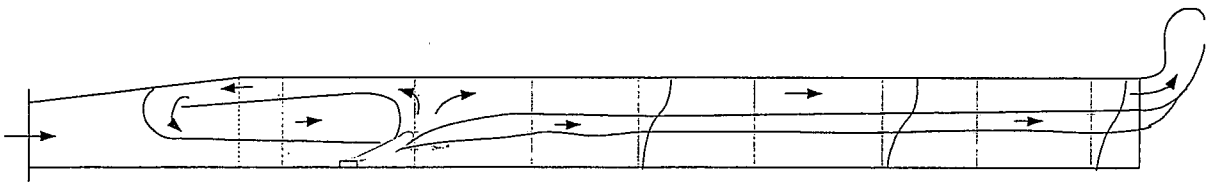

Figure 5c Longitudinal ventilation 0.75 m/s (2.1 m/s). Fire source 49.2 kW(8.9 MW) **(test 19).**

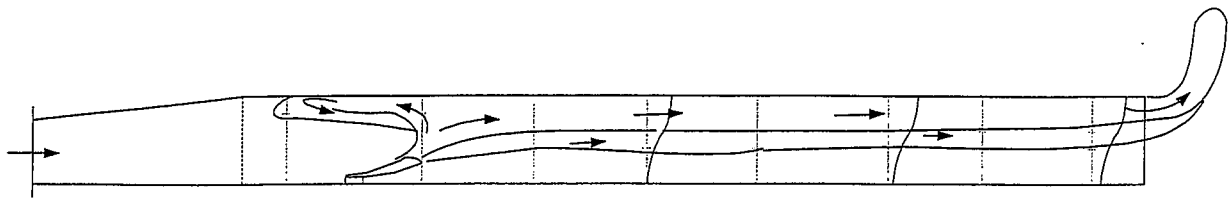

Figure 5d Longitudinal ventilation 1 m/s (2.8 m/s). Fire source 57.4 kW(10.4 MW) **(test 18).**

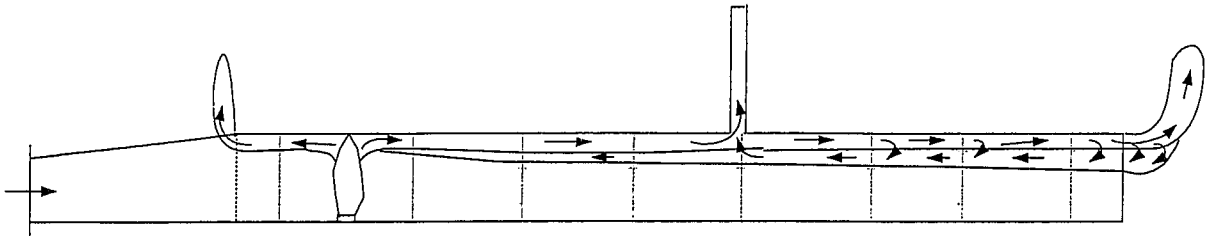

Figure 5e No longitudinal ventilation. One 0.4 x 0.4 m thermal shaft (3.2 x 3.2 m). Fire source 71.9 kW (13 MW) **(test 14).**

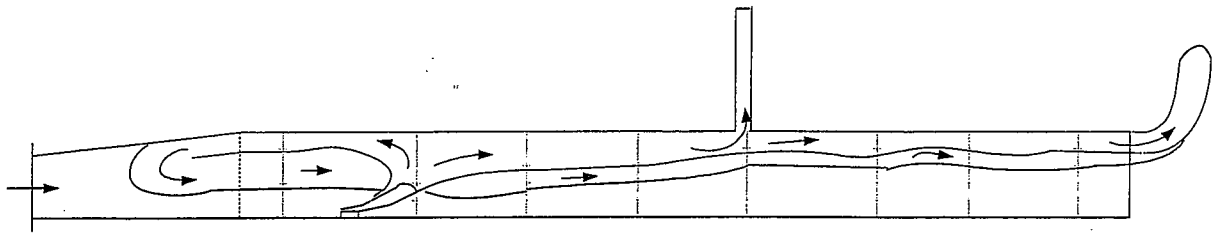

Figure 5f Longitudinal ventilation 0.75 m/s (2.1 m/s). One 0.4 x 0.4 m thermal shaft (3.2 x 3.2 m). Fire source 49 kW (8.9 MW). The height of the shaft was 3 m (24 m) **(test 12).**

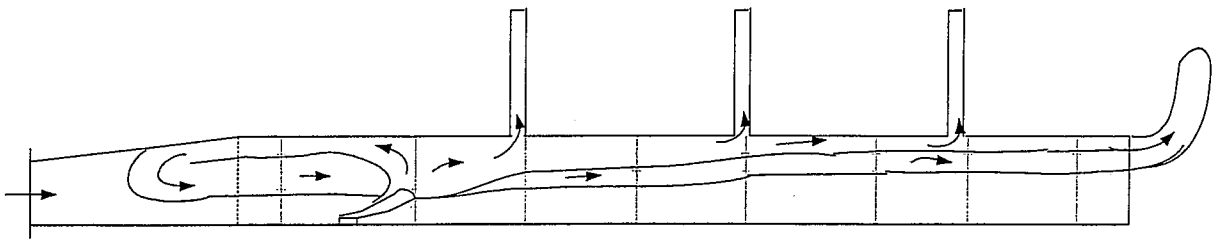

Figure 5g Longitudinal ventilation 0.75 m/s (2.1 m/s). Three 0.4 x 0.4 m thermal shafts (3.2 x 3.2 m). Fire source 46.6 kW (8.4 MW). The height was 3 m (24 m) **(test 10).**

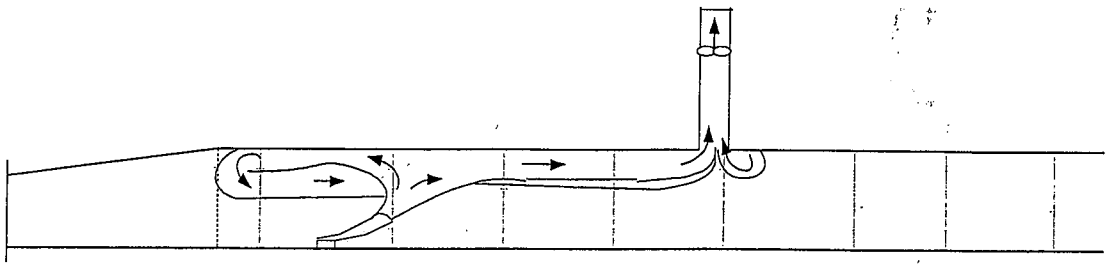

Figure 5h No longitudinal ventilation. Mechanical ventilation with exhaust flow of 2.7 m^3/s (488 m^3/s). The area of the shaft was 0.6 x 0.6 m (4.8 x 4.8 m) and the height was 2 m (16 m) (**test 28**). The smoke backlayering distance is 0.5 m from the exhaust opening.

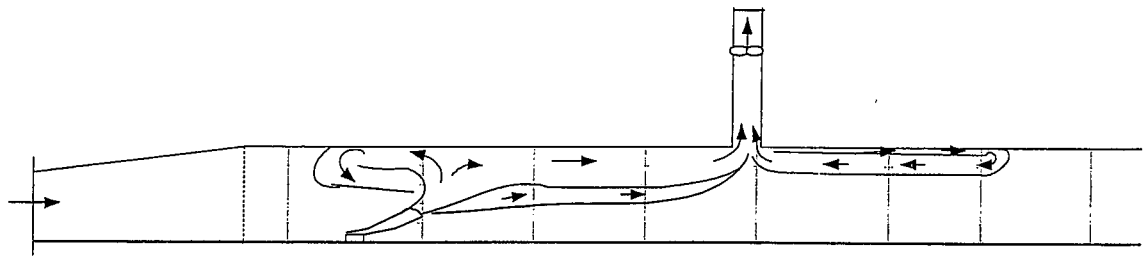

Figure 5i Longitudinal ventilation 1 m/s (2.8 m/s). Mechanical ventilation with exhaust flow of 2.7 m^3/s (488 m^3/s). The area of the shaft was 0.6 x 0.6 m (4.8 x 4.8 m) and the height was 2 m (16 m) (**test 29**). The smoke backlayering distance is 5.5 m from the exhaust opening.

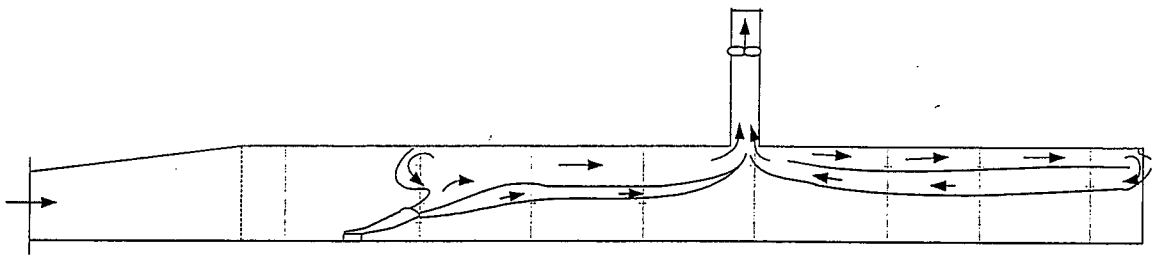

Figure 5j Longitudinal ventilation 2 m/s (5.6 m/s). Mechanical ventilation with exhaust flow of 2.7 m^3/s (488 m^3/s). The area of the shaft was 0.6 x 0.6 m (4.8 x 4.8 m) and the height was 2 m (16 m) (**test 36**). The smoke backlayering distance is 8.5 m from the exhaust opening.

There is a distinct difference between the efficiency of mechanical ventilation and thermal ventilation. The mechanical ventilation is able to stop the smoke spread downstream the exhaust opening (shaft) whereas the thermal shafts are not. The critical exhaust flow is 2.7 m^3/s (488 m^3/s) with no longitudinal velocity. Increasing the longitudinal velocity and maintaining the exhaust volume flow increase the backlayering distance of the smoke downstream the shaft. The backlayering distance downstream the mechanical shaft is given in Table 3. As can be seen in Table 3 the mechanical ventilation is very sensible for the longitudinal velocity. Increasing longitudinal velocity does not affect the efficiency of the mechanical ventilation (mass flow rate) but more smoke is pushed by the side of the exhaust opening. This results in more smoke downstream the exhaust opening. The conclusion is thus that the critical flow rate of the mechanical ventilation to prevent smoke spread downstream the shaft is highly dependent on the longitudinal velocity. Another parameter not tested here

is the geometrical area of the shaft. The geometrical area of the shaft may influence the results considerably.

Table 3 Backlayering distance of smoke downstream the mechanical shaft.

Test nr	Air velocity (m/s)	Exhaust ventilation (m^3/s)	Q (kW)	Backlayering distance (m)
27	0	2	61.62	1.5
28	0	2.7	45.03	0.5
29	1	2.7	59.64	5.5
30	1	1.56	56.49	>> 8.5***
31	1	2	56.09	> 8.5**
32	1	2.3	64.39	8.5*
33	0.5	2	53.33	5.5
34	1	2.7	59.25	5.5
35	2	2	74.26	>>8.5*
36	2	2.7	73.87	8.5

* ** >> smoke was flowing freely out from the tunnel end without any effects of the exhaust ventilation
** > smoke was flowing out from the tunnel end but smoke was sucked in again to the exhaust opening
* the smoke stopped at the tunnel end. Small quantities of smoke left the tunnel end.

From figures 5a-j we find that the thermal exhaust ventilation does not prevent the smoke spread downstream the exhaust opening in any experiment. In order to obtain similar efficiency as the mechanical ventilation the shafts must be built much higher. As an example the shaft must be at least 11 - 12 m high (88 - 96 m) in order to obtain similar volume flows as in the mechanical shaft.

The test data show that the longitudinal ventilation affects the thermal ventilation rate positively since mass flow rate in the shaft increases by increasing longitudinal ventilation. This can be observed in figure 9.

3.2 Smoke concentration

The smoke concentration (kg/m^3) is an important measure of the visibility in the tunnel. There is a correlation between smoke concentration and visibility in smoke. In figure 6 smoke concentration measured by optical density meters are plotted as a function of longitudinal velocity and type of ventilation shaft. The optical density per path length of smoke is converted into smoke concentration (kg/m^3) by divide the optical density by 3300 m^2/kg. In figure 6 we observe that when no shafts are present the smoke concentration reduces (improved visibility) with increasing longitudinal velocity. This is an interesting observation since this may improve the conditions for escaping people downstream the fire. Increasing velocity also reduces the temperature and the amount of toxic gases. On the other hand the heat release rate may be adversely affected for material with in-depth combustion (solid materials) so these effects may be cancelled. The heat release rate of pool fires may be either reduced or increased depending on the longitudinal velocity. These effects can be observed in figure 10.

Further, we observe that when shafts are present there is a slight tendency to increase the smoke concentration (reduction in visibility) with increasing velocity. The smoke concentration when using thermal shafts are, however, reduced considerably. Thus, thermal shafts will undoubtedly improve the visibility downstream the shaft.

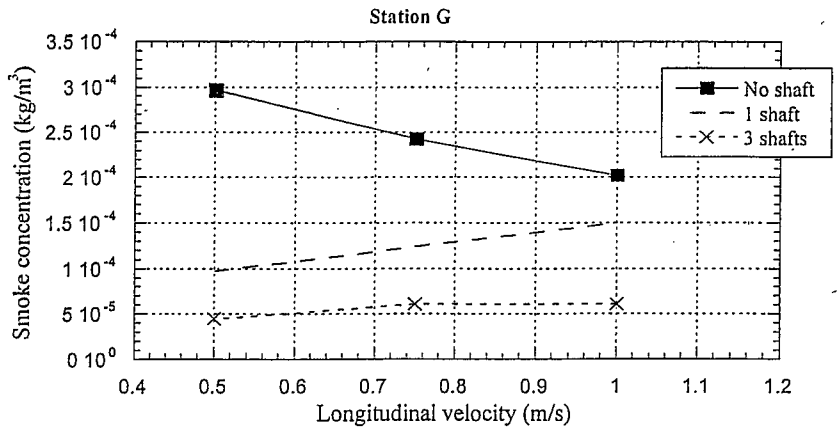

Figure 6 Measured smoke concentration in measuring point G, 16.5 m downstream the fire, for different longitudinal velocities and different thermal ventilation.

3.3 Gas temperature

3.3.1 Gas temperature profile

The effects of the longitudinal velocity on the temperature profiles is interesting since the smoke concentration can be expected to follow the temperature profile at each station. The temperature profiles have been plotted in figure 7a-c. Apparently there exist three main layers, a layer with high temperatures and dense smoke close to the ceiling, a mixing layer with intermediate temperatures and smoke density and a cold layer close to the floor with relatively small amount of smoke. If we compare the temperature profiles in figure 7a-c with the smoke profiles in figures 5a-d we find them very similar in shape. Thus, one would expect that the temperature profile has close relation with the smoke profile.

The gas temperature profiles were measured at locations E, F and G. In figure 7a-c the temperature profiles at 4 different longitudinal velocities 0, 0.5, 0.75 and 1 m/s (0, 1.4, 2.1, 2.8 m/s) are plotted for three different measuring points. Tests 17, 18, 19, 20 were used. No thermal shafts were present. Station E was located 6.5 m (52 m) downstream the fire, station F 11.5 m (92 m) and station G 16.5 m (132m).

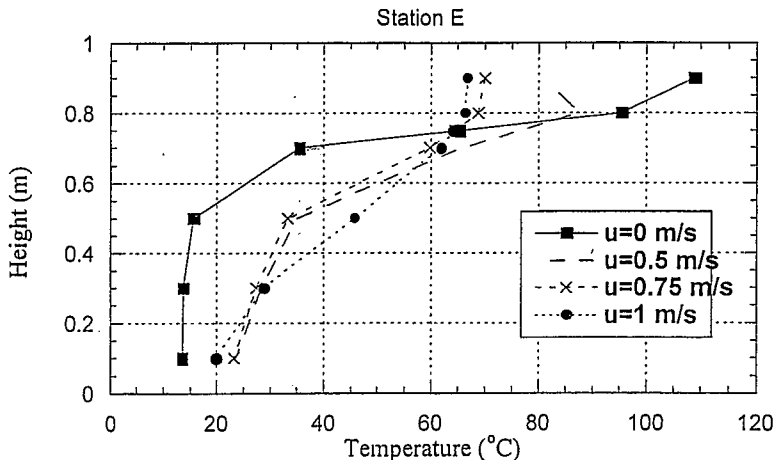

Figure 7a Temperature profiles for longitudinal ventilation at station E.

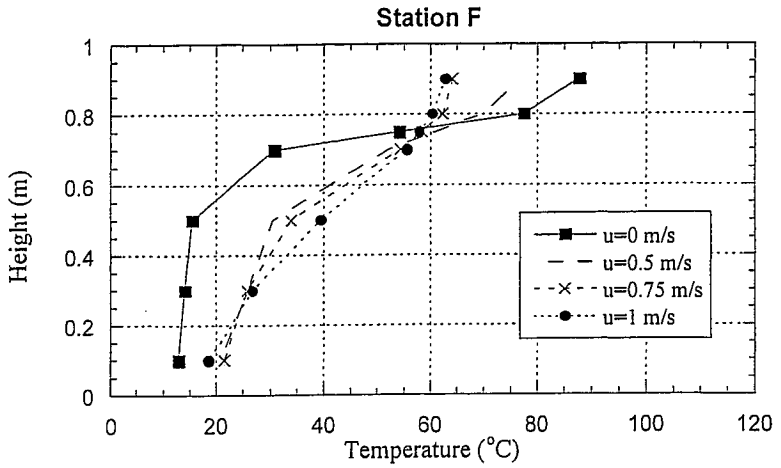

Figure 7b Temperature profiles for longitudinal ventilation at station F.

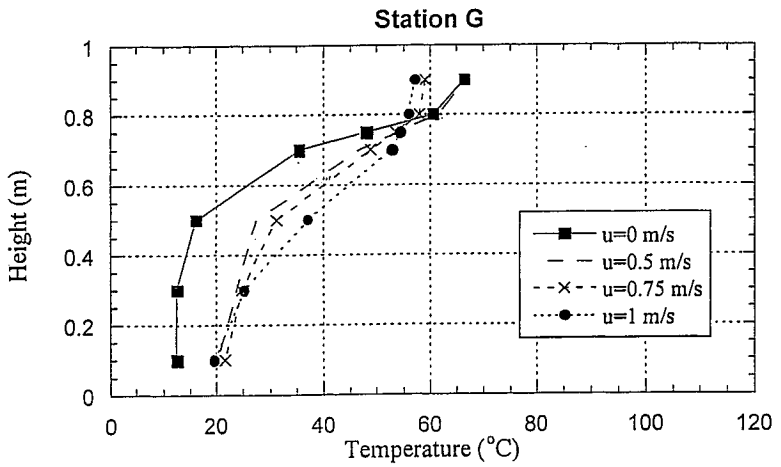

Figure 7c Temperature profiles for longitudinal ventilation at station G.

3.3.2 Gas temperature along the tunnel ceiling

The gas temperature along the ceiling is an interesting parameter for the fire safety of people escaping from tunnels. In figures 8a-d it is shown how the different ventilation arrangement affects the temperature distribution along the tunnel. The influence of longitudinal velocity without any shafts is also shown. The temperatures decay as a function of the distance from the fire. Over 50 % reduction of the gas temperature in the ceiling is obtained after 2 - 3 m (16 - 24 m) from the fire source. This is mainly due to the radiation losses to the surrounding walls. From 2.5 m and up to 20 m (20 - 160 m) the temperature reduction is not as steep as closer to the fire. The heat losses in this area are dominated by convection losses from the gas volume to the surrounding walls.

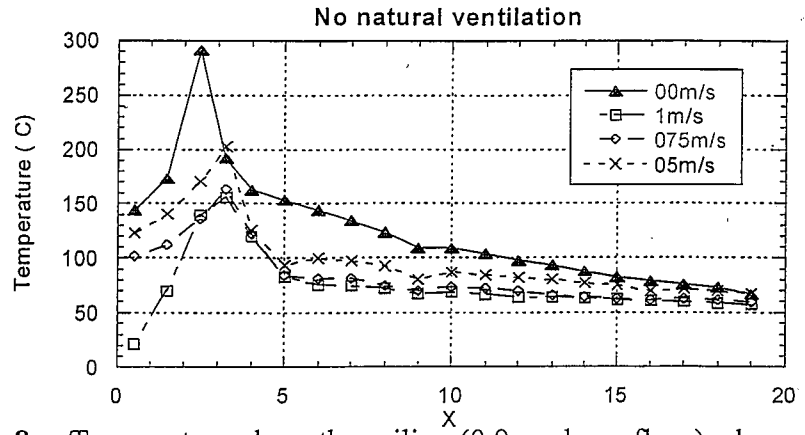

Figure 8a Temperature along the ceiling (0.9 m above floor) where x is the distance along the tunnel. The fire is located at x=2.5 m.

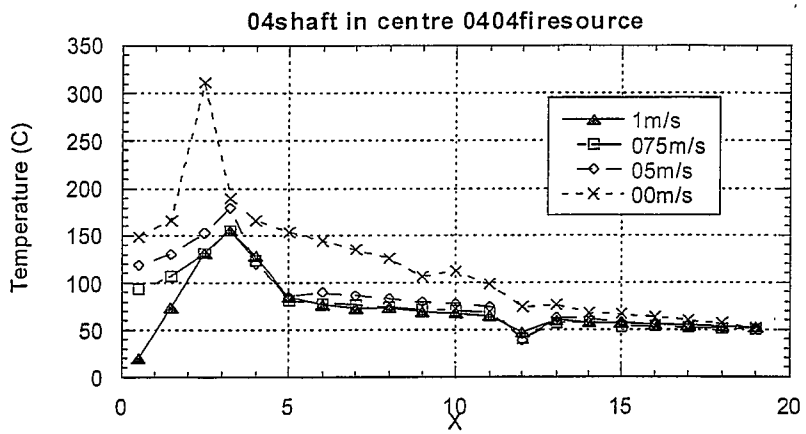

Figure 8b Temperature along the ceiling (0.9 m above floor) where x is the distance along the tunnel. The fire is located at x=2.5 m. One thermal shaft measuring 0.4 x 0.4 m and 3 m high is located in B. Fire source 0.4 x 0.4 m.

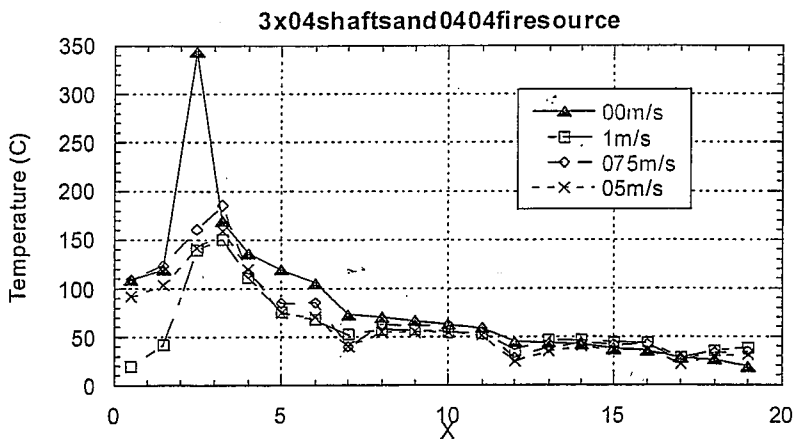

Figure 8c Temperature along the ceiling (0.9 m above floor) where x is the distance along the tunnel. The fire is located at x=2.5 m. Threethermalshafts measuring 0.4 x 0.4 m and 3 m high is located in A,B and C. Fire source 0.4 x 0.4 m.

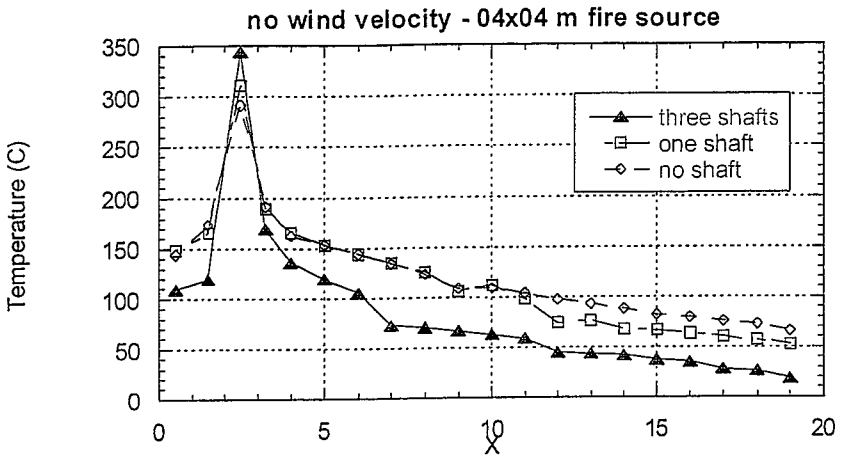

Figure 8d Temperature along the ceiling (0.9 m above floor) where x is the distance along the tunnel. The fire is located at x=2.5 m. No longitudinal ventilation. Fire source 0.4 x 0.4 m.

3.4 Mass flow rate of air in the shaft

The experimental results indicate that increased longitudinal velocity slightly increases the mass flow rate of smoke through the thermal shafts (see figure 9). The increase is not significant for the efficiency of the shafts but this tendency was not obtained with the mechanical ventilation where the mass flow rate was constant during all tests.

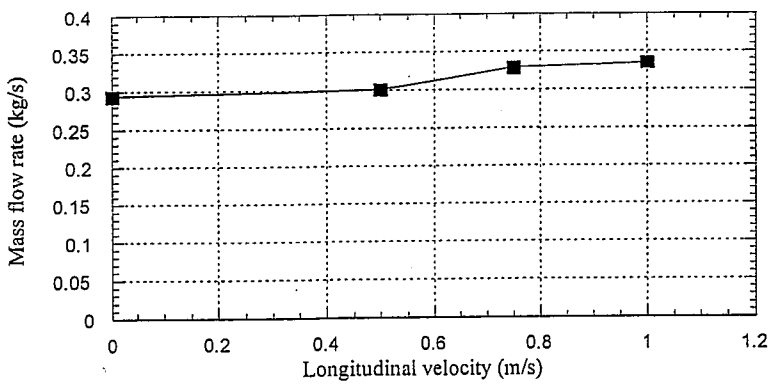

Figure 9 Measured mass flow rate in one thermal shaft with varying longitudinal velocity.

3.5 Mass burning rate of fuel

The effects of ventilation on the mass burning rate of pool fires have been investigated for the tests performed here. In figure 10 the mass burning rate per fuel area is plotted as a function of the longitudinal velocity. The tests show that the mass burning rate is highly dependent on the longitudinal velocity. The mass burning rate is highest when there is no longitudinal velocity in the tunnel. This is mainly due to the radiation feedback from the flame and surrounding walls. When the longitudinal velocity is increased the flame deflects and the radiation feedback to the fuel surface is reduced.

The lowest mass burning rates are obtained at 0.5 and 0.75 m/s (1.4 and 2.1 m/s) and then it increase again. At 1 m/s or higher the mass burning rate increase again, probably due increased diffusion at the fuel surface. These results are of great interest when considering ventilation effects on heat release rate in tunnels.

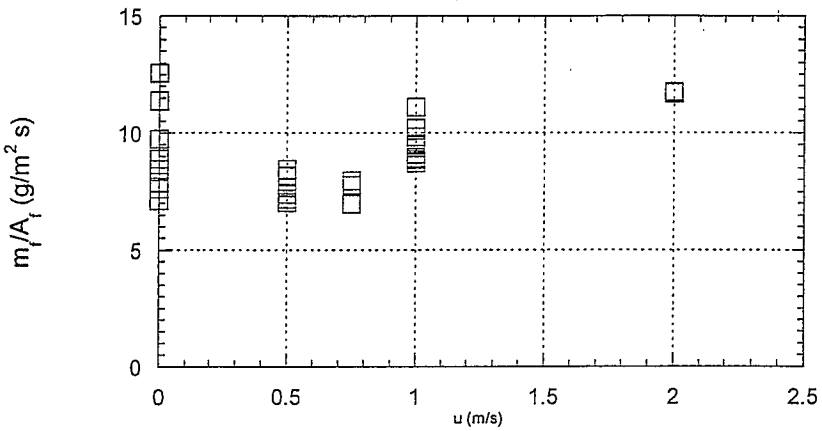

Figure 10 Mass burning rate per unit fuel area versus longitudinal velocity inside the tunnel.

3.6 Heat flux at ceiling

The total heat flux was measured at the ceiling with a Schmidt-Boelter gage which measures the total heat flux to the ceiling. The gage was placed flush to the ceiling at station E and at the centreline in the tunnel. The Schmidt-Boelter gage measures both the convective and radiative heat flux. As can be observed from figure 11 the heat flux to the ceiling is affected by the longitudinal velocity.

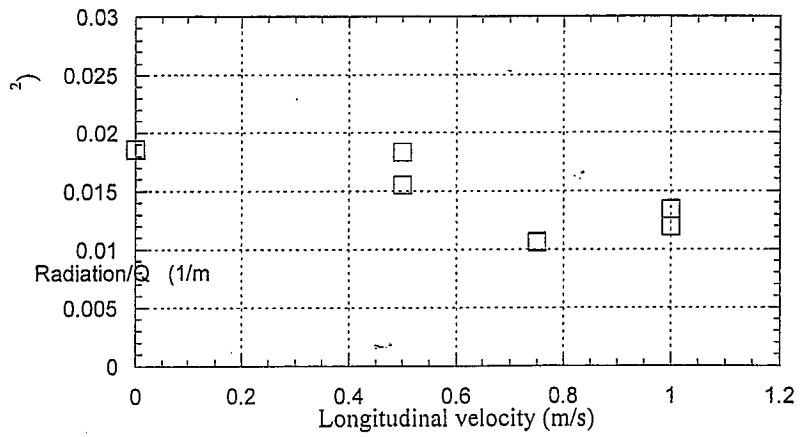

Figure 11 Total heat flux to the ceiling divided with the total heat release rate (Q) shown as a function of the longitudinal velocity. The heat flux was measured at station E and no shafts were present.

4 Conclusions

The report shows the influence of longitudinal ventilation on the smoke spread when using thermal and mechanical point exhaust ventilation in tunnels. The smoke spread and smoke concentration, both along the tunnel and over the cross section, is highly dependent on the type of exhaust ventilation and the longitudinal velocity.

The thermal exhaust ventilation did not prevent the smoke spread downstream the exhaust opening in any case whereas the mechanical ventilation did. The efficiency of the thermal shaft is highly dependent on the height of the shaft and the temperature inside the shaft.

The visibility was found to improve slightly with increasing longitudinal velocity when no shafts were present. The presence of thermal shafts did improve the visibility downstream considerably. The experiments also show that increased longitudinal velocity increases the efficiency of the thermal shafts whereas it had no effects on the mechanical ventilation. The critical flow rate of the mechanical ventilation, which prevents any smoke spread downstream the exhaust opening, is highly dependent on the longitudinal velocity.

5 References

1 Hägglund, B., Simulating fires in natural and forced ventilated enclosures, FOA Rapport C20637-2.4, Dec 1986, National Defence Research Institute,Sweden

2 Heskestad, G., Model study of automatic smoke and heat vent performance in sprinklered fires, Factory Mutual Research, September 1974.

3 Babrauskas, V., and Grayson, S., Heat Release in Fires, Elsevier Applied Science, 1992.

Appendix

In the following test results from tests with thermal and mechanical shafts are presented in tabulated form. The values are average values taken between 7th to 11th minute of the test.

Table 1 Results from tests with thermal and mechanical shafts.

Test no	U (m/s)	m_f (g/s)	Q (kW)	$m_{a,A}$ (kg/s)	$m_{a,B}$ (kg/s)	$m_{a,C}$ (kg/s)	OD_E (1/m)	OD_F (1/m)	OD_G (1/m)	$O2_E$ (%)	$O2_F$ (%)	$O2_G$ (%)
01	0.0	0.970	38.3	0.155	0.113	0.075	NA	0.41	0.75	20.71	20.68	20.44
02	1.0	1.071	42.3	0.176	0.192	0.187	NA	0.38	0.33	20.58	20.62	20.72
03	0.0	0.828	32.7	0.244	0.181	0.105	NA	0.34	0.05	20.88	20.74	20.93
04	0.5	0.781	30.9	0.309	0.217	0.168	NA	0.178	0.166	20.63	20.80	20.84
05	0.75	0.757	29.9	0.313	0.235	0.201	NA	0.230	0.147	20.63	20.69	20.79
06	1.0	1.036	40.9	0.303	0.259	0.243	NA	0.309	0.222	20.59	20.72	20.73
07	0.0	1.353	53.4	0.268	0.200	0.116	NA	0.488	0.209	20.82	20.61	20.83
08	1.0	1.391	54.9	0.342	0.290	0.259	NA	0.308	0.201	20.51	20.69	20.75
09	0.75	1.273	50.3	0.368	0.258	0.213	NA	0.210	0.201	20.79	20.80	20.79
10	0.5	1.179	46.6	0.378	0.274	0.228	NA	0.178	0.147	20.61	20.71	20.82
11	0.5	1.233	48.7	-	0.301	-	NA	0.244	0.321	20.35	20.86	20.74
12	0.75	1.241	49.0	-	0.329	-	NA	0.338	0.409	20.33	20.59	20.60
13	1.0	1.494	59.0	-	0.335	-	NA	0.480	0.494	20.31	20.51	20.59
14	0.0	1.820	71.9	-	0.294	-	NA	0.799	1.27	20.67	20.23	19.99
15	0.5	1.224	48.3	-	0.100	-	0.654	0.486	0.569	20.22	20.66	20.56
16	1.0	1.772	70.0	-	0.094	-	0.558	0.608	0.629	20.56	20.55	20.44
17	0.0	2.011	79.4	-	-	-	0.557	0.927	1.423	20.39	20.20	20.01
18	1.0	1.452	57.4	-	-	-	0.656	0.630	0.677	20.34	20.40	20.39
19	0.75	1.246	49.2	-	-	-	0.740	0.758	0.801	20.28	20.25	20.30
20	0.5	1.311	51.8	-	-	-	0.960	0.879	0.979	20.12	20.15	20.28
21	0.0	0.859	33.9	-	-	-	0.522	0.342	0.501	20.78	20.75	20.57
22	1.0	1.039	41.0	-	-	-	0.476	0.475	0.494	20.58	20.57	20.61
23	0.75	0.757	29.9	-	-	-	0.473	0.468	0.493	20.55	20.53	20.59
24	0.5	0.767	30.3	-	-	-	0.669	0.660	0.667	20.38	20.33	20.52
25	0.5	1.299	51.3	-	0.560	-	0.703	0.328	0.512	20.36	20.65	20.63
26	1.0	1.414	55.9	-	0.752	-	0.588	0.288	0.333	20.34	20.53	20.69

Test no	U (m/s)	m_f (g/s)	Q (kW)	$m_{a,A}$ (kg/s)	$m_{a,B}$ (kg/s)	$m_{a,C}$ (kg/s)	OD_E (1/m)	OD_F (1/m)	OD_G (1/m)	O_{2E} (%)	O_{2F} (%)	O_{2G} (%)
27	0	1.56	61.62	-	2.17	-	0.226	0.015	0.015	20.95	20.77	20.95
28	0	1.14	45.03	-	3.05	-	0.535	0.014	0.013	20.95	20.48	20.84
29	1	1.51	59.64	-	2.98	-	0.575	0.270	0.003	20.71	20.30	20.95
30	1	1.43	56.49	-	1.63	-	0.541	0.250	0.233	20.67	20.36	20.73
31	1	1.42	56.09	-	2.08	-	0.532	0.224	0.260	20.78	20.36	20.75
32	1	1.63	64.39	-	2.42	-	0.548	0.279	0.330	20.71	20.38	20.68
33	0.5	1.35	53.33	-	2.13	-	0.656	0.577	0.004	20.49	20.20	20.95
34	1	1.50	59.25	-	2.93	-	0.531	0.246	0.001	20.78	20.35	20.95
35	2	1.89	74.26	-	2.14	-	0.464	0.200	0.227	20.89	20.53	20.95
36	2	1.87	73.87	-	2.95	-	0.545	0.223	0.245	20.87	20.51	20.95

U = Velocity
m_f = Mass loss rate of fuel
Q = Heat realise rate
m_a = Mass flow rate of air
OD= Optical dencisity
O_2 = Oxygen concentration

Table 2 The gas temperature 0.9 m below ceiling.

Test no	0.5 m	1.5 m	2.5 m	3.2 m	4 m	5 m	6 m	7 m	8 m	9 m	10 m	11 m	12 m	13 m	14 m	15 m	16 m	17 m	18 m	19 m
01	84,0	79,0	283,2	129,4	107,6	85,9	87,8	60,4	59,2	48,3	52,4	48,9	36,7	37,1	28,2	31,7	29,6	23,2	23,1	19,2
02	15,4	21,7	73,0	103,5	79,5	55,7	53,3	42,8	47,8	44,9	46,6	45,1	35,3	41,1	37,8	40,3	39,6	30,2	35,2	34,4
03	80,7	83,1	262,7	125,5	103,0	80,1	82,3	57,3	55,9	44,4	50,2	46,0	34,5	34,0	26,3	29,0	27,6	21,2	16,4	14,2
04	76,9	85,4	105,9	113,7	81,0	56,6	58,8	36,8	47,0	41,6	45,3	42,8	27,0	34,8	30,5	33,1	33,5	20,8	28,0	25,8
05	59,6	72,9	100,8	106,5	79,0	53,3	51,4	37,6	44,0	40,1	43,2	41,2	26,0	33,7	30,9	33,1	33,0	22,0	26,1	26,4
06	18,8	25,8	80,5	106,7	84,2	61,2	55,1	43,4	48,3	49,4	47,4	45,8	34,1	41,2	42,4	40,0	39,4	28,7	34,1	36,2
07	109,6	119,0	343,1	169,3	135,9	119,4	105,1	72,9	69,8	66,9	63,0	59,0	44,6	43,8	42,2	37,6	35,9	28,4	25,9	19,2
08	19,6	41,7	139,1	150,5	110,6	75,2	67,4	52,0	57,5	56,7	55,1	53,8	36,0	45,9	46,5	44,1	43,8	28,2	35,3	38,2
09	109,2	123,3	160,4	185,3	116,0	85,1	85,4	39,8	62,8	61,0	62,0	58,6	28,0	38,0	43,4	41,4	42,4	25,8	33,4	34,0
10	91,6	103,4	141,5	158,7	119,1	74,2	69,8	39,9	54,9	55,1	54,3	51,7	24,9	34,8	39,4	36,5	37,2	21,7	30,2	31,6
11	118,6	130,1	152,5	179,3	120,2	84,6	89,1	86,4	83,0	79,7	77,7	75,1	39,2	63,1	61,2	57,9	55,9	54,5	53,1	51,3
12	93,1	106,6	130,7	155,2	123,3	81,2	77,8	77,0	74,2	71,8	70,1	68,9	41,2	57,3	58,3	53,3	53,8	52,4	51,6	50,0
13	20,4	73,5	131,2	155,4	128,1	84,8	76,6	72,6	73,7	68,7	67,3	65,1	47,5	59,8	58,5	56,8	55,7	54,6	53,3	51,8
14	148,9	166,1	310,7	189,0	166,1	152,9	144,2	134,4	124,9	106,2	112,2	98,2	74,3	76,2	67,2	66,8	63,2	59,9	56,7	52,7
15	117,3	129,1	156,1	176,7	123,5	84,6	86,9	87,0	83,2	74,4	77,8	75,7	64,3	68,8	66,3	63,8	61,9	60,5	59,0	56,9
16	18,8	67,8	134,6	150,2	119,5	82,1	73,6	72,1	70,9	64,7	66,6	65,0	60,2	61,8	60,5	59,0	57,8	56,8	55,6	54,0
17	144,0	173,2	291,3	191,6	162,6	153,2	144,0	133,9	123,4	108,9	109,2	103,8	97,6	92,8	87,7	82,4	79,1	75,5	72,7	66,4
18	21,0	69,5	139,4	155,9	120,1	83,0	75,3	74,2	72,3	66,8	68,3	66,6	63,3	64,0	62,8	61,7	60,6	59,5	58,4	57,1
19	101,5	111,9	136,1	163,2	122,1	84,2	81,5	81,3	74,6	70,0	73,2	72,0	69,6	65,7	64,1	62,4	61,2	62,5	61,0	59,0
20	122,7	139,7	170,6	202,5	125,8	94,0	100,0	97,1	92,6	80,8	86,7	84,7	82,0	79,9	76,9	74,9	69,0	71,3	69,6	66,8
21	85,2	86,1	261,1	132,4	117,6	102,3	98,4	89,7	75,8	63,5	70,0	65,8	60,9	58,2	53,5	51,5	49,3	47,0	45,1	42,4
22	16,5	21,9	73,6	99,6	83,3	60,2	56,3	55,6	55,0	50,2	53,1	51,9	50,4	49,9	49,1	48,3	47,8	47,1	46,5	45,6
23	56,2	70,5	98,2	100,9	80,6	58,1	54,0	55,0	54,0	47,5	50,2	49,0	47,8	47,2	47,6	46,9	46,2	45,6	44,9	43,7
24	86,9	92,4	107,1	122,9	87,0	65,0	64,7	64,0	61,6	56,3	60,6	59,6	57,7	54,0	54,7	53,8	51,5	51,8	51,1	49,6
25	127,5	141,9	167,8	197,0	124,4	95,0	99,5	96,4	91,6	90,0	86,6	83,6	35,4	57,8	55,1	53,8	53,2	52,2	49,2	49,1
26	21,9	67,3	150,0	153,7	126,5	86,6	79,5	78,6	76,6	75,5	72,9	70,7	33,2	50,2	53,9	54,8	52,8	48,5	49,5	48,6

Table 2 The gas temperature 0.9 m below ceiling.

Test no	0.5 m	1.5 m	2.5 m	.2 m	4 m	5 m	6 m	7 m	8 m	9 m	10 m	11 m	12 m	13 m	14 m	15 m	16 m	17 m	18 m	19 m
27	129	142	187	209	130	117	115	107	100	97	94	85	35	21	18	18	18	18	18	19
28	103	114	129	150	102	75	77	74	68	68	69	65	21	17	17	18	18	18	18	18
29	23	68	146	159	130	88	81	80	78	72	75	71	28	32	32	31	29	22	20	20
30	24	61	155	160	124	85	78	80	78	73	74	71	30	40	43	41	40	40	38	37
31	21	69	147	154	120	82	75	74	73	69	70	66	25	30	32	32	32	32	31	30
32	21	71	143	157	127	87	77	76	77	72	73	69	24	29	32	31	31	31	30	29
33	131	144	173	200	127	93	101	97	93	85	89	86	43	46	39	38	28	19	19	19
34	24	68	148	161	126	85	78	76	74	73	70	69	24	27	28	28	27	23	17	17
35	15	15	25	57	96	70	59	58	58	58	59	55	23	29	30	31	30	30	29	28
36	16	17	34	76	112	78	67	64	64	64	65	64	25	29	28	27	27	27	26	26

Table 3 The vertical gas temperature at station D, and E

Test no	D 0.9 m	D 0.8 m	D 0.7 m	D 0.5 m	D 0.3 m	D 0.1 m	E 0.9 m	E 0.8 m	E 0.7 m	E 0.5 m	E 0.3 m	E 0.1 m
01	85,9	42,0	25,7	17,0	15,9	15,1	48,3	24,3	16,1	14,8	14,4	13,8
02	55,7	48,3	39,8	30,1	23,4	18,1	44,9	45,7	39,9	30,9	23,6	18,0
03	80,1	40,9	26,4	18,5	17,7	15,8	44,4	22,4	16,0	15,1	14,6	14,0
04	56,6	46,7	33,5	25,9	23,2	20,7	41,6	42,0	29,0	21,4	20,5	18,6
05	53,3	45,3	36,4	28,2	23,9	20,7	40,1	40,8	30,9	22,8	21,2	20,3
06	61,2	51,9	45,7	34,1	27,2	21,2	49,4	46,5	45,0	36,6	27,3	21,0
07	119,4	61,7	38,2	23,9	23,3	21,2	66,9	32,3	21,0	20,0	19,3	18,7
08	75,2	61,3	52,1	37,0	28,9	21,6	56,7	54,5	49,8	36,5	25,9	20,7
09	85,1	71,7	50,6	32,5	30,1	22,7	61,0	41,0	28,7	23,5	21,0	15,6
10	74,2	57,4	47,0	34,6	29,4	22,5	55,1	45,4	34,5	25,3	22,7	20,1
11	84,6	68,4	44,2	30,9	29,9	22,4	79,7	77,2	60,4	29,1	23,3	19,3
12	81,2	61,9	47,0	33,9	31,1	23,7	71,8	69,2	57,1	32,2	26,3	22,9
13	84,8	66,4	52,7	37,4	29,3	21,4	68,7	66,4	62,3	44,5	27,6	20,0
14	152,9	122,9	38,1	21,2	17,9	19,7	106,2	83,9	27,6	16,8	17,5	15,2
15	84,6	69,5	46,0	32,4	27,2	24,4	74,4	76,6	57,7	28,6	24,5	20,7
16	82,1	64,7	51,9	36,5	27,3	19,6	64,7	63,3	59,8	44,1	27,0	18,4
17	153,2	119,4	45,3	20,7	21,9	17,0	108,9	95,3	35,4	15,5	13,7	13,6
18	83,0	65,6	53,5	37,5	30,7	22,3	66,8	66,3	61,9	45,8	28,8	19,9
19	84,2	64,5	50,3	36,0	30,0	25,7	70,0	68,8	59,8	33,3	27,3	23,2
20	94,0	77,8	52,2	36,0	31,2	26,6	80,8	87,4	65,9	35,0	28,3	23,5
21	102,3	45,5	29,6	23,0	18,2	18,7	63,5	43,7	23,5	18,0	16,7	16,1
22	60,2	49,8	42,0	30,9	24,9	20,7	50,2	51,9	48,0	38,7	27,3	19,0
23	58,1	46,9	39,9	30,3	24,9	22,5	47,5	50,8	45,2	32,6	25,1	20,6
24	65,0	51,2	39,8	29,9	26,8	23,9	56,3	60,8	54,4	33,1	25,9	21,4
25	95,0	81,5	50,5	33,6	29,1	29,6	90,0	82,5	48,0	29,1	25,3	20,1

Test no	D 0.9 m	D 0.8 m	D 0.7 m	D 0.5 m	D 0.3 m	D 0.1 m	E 0.9 m	E 0.8 m	E 0.7 m	E 0.5 m	E 0.3 m	E 0.1 m
27	26	29	34	67	101	117	22	24	25	35	78	97
28	24	26	28	44	59	75	22	23	26	48	66	68
29	26	32	42	58	71	88	24	32	50	66	71	72
30	28	34	43	58	69	85	25	34	49	66	69	73
31	24	31	38	53	65	82	22	30	46	62	64	69
32	25	33	40	56	69	87	22	31	47	64	66	72
33	32	35	37	53	80	93	24	28	33	56	78	85
34	26	34	42	57	70	85	23	31	46	62	65	73
35	23	28	37	50	58	70	21	28	38	49	52	58
36	25	32	42	57	66	78	23	31	42	55	58	64

Table 3 The vertical gas temperature at station F and G.

Test no	F 0.9 m	F 0.8 m	F 0.7 m	F 0.5 m	F 0.3 m	F 0.1 m	G 0.9m	G 0.8 m	G 0.7 m	G 0.5 m	G 0.3 m	G 0.1 m
01	28,2	21,8	15,6	14,6	14,1	13,9	19,2	19,4	16,2	14,5	13,9	13,7
02	37,8	38,9	34,8	27,8	20,9	17,5	34,4	33,5	27,7	23,1	18,9	17,2
03	26,3	21,4	16,0	14,2	13,9	13,7	14,2	14,0	14,0	13,8	13,7	13,6
04	30,5	26,3	19,7	18,3	16,8	15,8	25,8	22,7	17,8	16,4	15,9	15,9
05	30,9	31,2	24,7	21,3	19,6	18,3	26,4	24,4	20,3	18,9	17,5	16,4
06	42,4	37,9	35,7	28,9	23,7	20,5	36,2	32,6	30,2	24,7	21,7	20,1
07	42,2	28,8	21,9	18,7	18,4	18,1	19,2	18,7	18,5	18,2	18,0	17,8
08	46,5	41,3	34,9	26,9	22,1	20,2	38,2	33,5	28,5	23,0	21,0	20,0
09	43,4	30,5	22,5	18,9	16,0	14,9	34,0	26,1	21,6	16,3	14,7	14,6
10	39,4	31,3	24,6	21,1	19,0	13,8	31,6	24,4	22,1	18,8	14,8	13,0
11	61,2	36,8	24,4	21,1	19,3	14,8	51,3	34,5	26,6	21,3	17,4	14,3
12	58,3	50,7	36,2	25,4	23,1	21,2	50,0	42,8	33,4	24,8	22,4	20,4
13	58,5	53,2	46,0	31,7	22,7	18,6	51,8	47,7	41,0	28,7	21,8	18,9
14	67,2	59,0	28,9	17,7	15,8	14,9	52,7	47,7	38,2	20,5	14,3	14,1
15	66,3	50,6	28,5	23,2	21,4	16,1	56,9	46,9	34,3	23,1	19,4	14,9
16	60,5	55,4	51,1	37,0	24,9	17,1	54,0	53,4	49,0	33,5	23,2	18,1
17	87,7	77,4	30,7	15,4	14,0	12,8	66,4	60,5	35,4	16,2	12,4	12,4
18	62,8	60,3	55,5	39,4	26,8	18,5	57,1	55,8	52,8	37,0	25,3	19,6
19	64,1	62,2	54,3	33,9	25,8	21,4	59,0	57,9	48,9	31,2	24,8	21,6
20	76,9	69,7	52,1	30,4	25,8	20,8	66,8	61,4	46,7	27,4	23,7	20,2
21	53,5	42,1	20,7	17,2	16,5	16,1	42,4	35,7	21,9	16,5	16,1	16,0
22	49,1	47,4	43,3	33,8	25,1	19,0	45,6	44,1	40,4	30,5	23,6	19,4
23	47,6	45,2	41,1	30,9	24,3	19,8	43,7	43,4	39,8	28,4	23,4	20,4
24	54,7	52,7	45,3	30,2	24,1	20,7	49,6	46,1	38,3	25,3	22,4	21,2
25	55,1	44,8	28,1	22,8	20,6	19,2	49,1	43,6	31,8	21,8	20,1	19,5
26	53,9	47,4	37,5	27,9	24,7	23,2	48,6	42,3	35,3	27,0	24,9	23,4

Test no	F 0.9 m	F 0.8 m	F 0.7 m	F 0.5 m	F 0.3 m	F 0.1 m	G 0.9m	G 0.8 m	G 0.7 m	G 0.5 m	G 0.3 m	G 0.1 m
27	18	18	18	18	18	18	17	18	18	18	18	19
28	17	17	17	17	17	17	17	17	17	18	18	18
29	20	20	22	27	31	32	20	20	20	20	20	20
30	25	26	29	34	38	43	21	23	25	29	32	37
31	16	20	24	26	29	32	16	16	19	25	28	30
32	16	18	24	27	31	32	16	16	20	25	28	29
33	18	19	21	29	37	39	18	18	18	19	19	19
34	17	17	19	24	27	28	16	16	16	17	17	17
35	21	22	23	24	26	30	15	20	22	24	26	28
36	14	21	24	25	27	28	13	14	19	24	25	26

Table 4 Gas temperatures in the shafts.

Test no	Temperature shaft A (°C)	Temperature shaft B (°C)	Temperature shaft C (°C)	Radiation station E (kW/m²)
01	42,3	27,8	18,8	0,7
02	48,4	40,2	34,0	0,4
03	32,0	24,2	17,5	0,5
04	44,2	29,4	22,5	0,4
05	43,1	32,0	24,2	0,35
06	48,3	40,8	32,9	0,39
07	42,0	31,8	22,8	0,64
08	58,8	47,7	34,3	0,57
09	54,9	34,6	24,8	0,78
10	53,5	35,0	23,6	0,66
11	-	44,7	-	0,83
12	-	50,0	-	0,71
13	-	56,8	-	0,69
14	-	48,3	-	1,31
15	-	64,8	-	1,03
16	-	56,3	-	0,87
17	-	-	-	1,48
18	-	-	-	0,77
19	-	-	-	0,52
20	-	-	-	0,95
21	-	-	-	0,63
22	-	-	-	0,49
23	-	-	-	0,32
24	-	-	-	0,47
25	-	39,7	-	1,05
26	-	56,5	-	0,74

Test no	Temperature shaft A (°C)	Temperature shaft B (°C)	Temperature shaft C (°C)	Radiation station E (kW/m²)
27	-	24	-	1,2
28	-	19	-	0.7
29	-	28	-	0.8
30	-	43	-	0.7
31	-	31	-	0.7
32	-	28	-	0.7
33	-	25	-	0.8
34	-	25	-	0.7
35	-	44	-	0.6
36	-	36	-	0.6